Advances in Science and Technology Research Journal

Advances in Science and Technology Research Journal 2023, 17(2), 279–288
https://doi.org/10.12913/22998624/161278
ISSN 2299–8624, License CC-BY 4.0

Received: 2022.12.30
Accepted: 2023.03.15
Published: 2023.04.01

Analysis of Flow-Induced Vibrations in a Heat Exchanger Tube Bundle Subjected to Variable Tube Flow Velocity

Akmal Hafeez[1*], Shahab Khushnood[2], Luqman Ahmad Nizam[3], Muhammad Usman[4], Muhammad Mohsin Rashid[4], Hasan Farid Khan[4], Muhammad Ayub[4], Adeel Qadir[4]

[1] Department of Mechanical and Aeronautical Engineering, University of Engineering and Technology (UET), Taxila, 47080, Pakistan
[2] Department of Mechanical Engineering, University of Wah, Wah Cantonment 47040, Pakistan
[3] Department of Mechanical Engineering, HITEC University, Taxila, Rawalpindi, Punjab 47080, Pakistan
[4] Department of Mechanical engineering, The University of Lahore, Lahore 54000, Pakistan
* Corresponding author's e-mail: mianakmal77@gmail.com

ABSTRACT
Tube bundles of shell and tube-type heat exchangers often fail because of vibrations produced in tubes due to flow. The turbulence in the flow is the primary cause of vibrations in the tubes. In this study, a tube positioned in the third row of the tube bundle was considered to determine the vibrational response of the heat exchanger tubes. The tube bundle was parallelly arranged in a triangular (60°) configuration having a pitch to diameter (P/D) ratio of 1.44. The internal tube flow velocity ranges from 0 to 0.371 m/s and the shell side velocity ranges from 0.5 m/s to 2 m/s. The experimentation shows that the amplitude of vibration without flow inside the tube is less as compared to the amplitude with the flow. Furthermore, as the velocity of internal tube flow escalates; the amplitude of tube vibrations tends to escalate as well even when the shell side flow velocity is kept constant. The data points from experiments tend to reside in the unstable region of the stability map and particularly on the map's left side, although the tube shows stable vibration behaviour as confirmed by the experimental results. Thus, further, development can be done by modifying the theoretical models to predict the realistic stability behaviour of tubes with internal tube flow.

Keywords: Cross-flow; parallel-triangular configuration; internal tube flow; damping; glass tube heat exchanger.

INTRODUCTION

Flow-induced vibrations (FIV) are a primary concern while designing the heat exchanger tube bundle. The main purpose to conduct this study was to understand the tube failure patterns against different tube and shell side flow velocities as well as no-flow conditions. The observations and results of this study shall act as guidelines for a safer heat exchanger design and consequently helps in avoiding the currently prevailing failure modes in heat exchanger operation. The different mechanisms that act as excitation sources to cause tubular vibrations in the heat exchangers are turbulence, vortex-induced instability, acoustic resonance, and fluid elastic instability [1] but the acoustic resonance is not considerable for single-phase liquid flow because this source of excitation is more significant in multi-phase flow and the gas flows. As the chances of failure in tube bundles due to FIV are quite higher, thus it is a prime concern for the designers and engineers to study this phenomenon in detail. In a single-span tube bundle, support is provided using baffle plates to each tube just like the tube sheets are supported in multi-span tube bundles. The designer's concern is to identify the natural frequency of the tube bundle and the severity of vibrations in it. This research has been carried out to study flow-induced vibrations to analyze their

effects so that the research results can be used in better designing as well as in industrial applications of heat exchangers. Price [2] observed that the instability of the flow causes tube vibrations which further disturbs the flow patterns and consequently enhances the tube displacements. Fluid-elastic instability occurs, as the displacement tends to increase. Chen [3] presented a general review of stability maps and established dissimilar instability models based on published experimental data and analytical models. Robert [4] was a pioneer in observing that the tube displacements caused dynamic tube row instability in the cross-flow. He investigated the movement of alternating tubes inside tube row and found that this motion produces a wake region in the downstream flow.

The completion of each flow cycle leads to a network of tube movements. Thus, the low clearance among tubes of the bundle produces the jet-switching phenomenon among strongly stacked tube bundles. Cross-flow methods have been used by researchers to numerically simulate the elastic instability of fluid from multiple cylinders [5].

The vibrations due to the fluid-elastic mechanism appear in many cylinders. The amplitude of these vibrations becomes quite large as the shell side velocity exceeds a critical point. Additionally, after surpassing this point the cylinders tend to exhibit vibrations in elliptical trajectories. Connor [6] evaluated different vibrating models for predicting instability and found that the model suggesting elliptical vibrations is more accurate. It depicts that both the cross-flow and streamwise flow directions should satisfy the energy balance as indicated the Eq. 1.

$$\frac{V_{pc}}{f_n D} = K\left(\frac{m\delta}{\rho D^2}\right)^{0.5} \tag{1}$$

where: K is the Connors' factor,
f_n is the natural frequency of the tube,
m is the mass ratio,
δ is log decrement,
ρ is the fluid density,
D is the external tube diameter and
V_{pc} is the gap/pitch velocity; it is determined using Eq. 2 [6] given below:

$$V_{pc} = \frac{VP}{P - D} \tag{2}$$

where: V represents shell side velocity, and
P is the tube bundle pitch. Blevins [7] further refined Connor's model to illustrate flow-dependent fluid damping. It is presented in Eq. 3

$$\frac{V_{pc}}{f_n D} = K\left[\left(\frac{m\delta}{\rho D^2}\right)2\pi\left(\zeta_x\zeta_y\right)^{0.5}\right]^{0.5} \tag{3}$$

where: ζ_x and ζ_y are the factor damping ratios in the x and y directions respectively. Blevins [7] found that the damping factors in the tube bundle play a complex role in fluid-elastic instability prediction.

The forced vibrations that are produced because of transient fluid forces are termed turbulence buffets. Turbulent flow can be categorized by the flow pattern variations as well as fluid velocity changes through the tubes [8]. The researchers have investigated unstable flow in the triangular tube bundle arrangement using flow visualization techniques and hot wire anemometry [9]. The tube bundle had a P/D ratio of 1.26 and Reynold's number ranged from 7.5×10^3 to 4.4×10^4. Observations revealed that coalescent jets were formed by the flow between the tunnel gaps. The change in the direction of flow occurred in a few cases as a metastable phenomenon. The turbulence features of the third last, fourth and fifth rows were close to the expected results. The primary source of excitation was the cross-flow of the excited vortices. A series of vortices was created because of fluid flow through the tube. These vortices generated quite a large amplitude of vibrations in the tube because of alternating forces. The vortex shedding frequency in the case of cross-flow from a single tube is defined using the relationship in Eq. (4) [8].

$$f_{vs} = \frac{StU}{d_\circ} \tag{4}$$

Where f_{vs} represents vortex shedding frequency, U depicts fluid velocity, St represents Strouhal number and d_o is the outside diameter of the cylinder. In recent decades, several researchers have inspected the vortex-shedding phenomenon. An experimental study was carried out to investigate the effects of the incident

flow angle on vibration behaviour in heat exchanger tube bundles [10]. Ali N et al [11] experimentally investigated the internal tube flow effect on the vibration response of tubes in a shell and tube heat exchanger. B. Grotz and F. Arnold [12] developed a relationship between tube spacing ratios and vortex shedding frequencies. It was found that the Strouhal number along with the vortex shedding frequency is a key feature of tube arrangement in the tube bundle [13]. The hypothesis indicates that periodic wave shedding induces fluctuating forces depending on several aspects such as fluid density, geometric structure of tube bundles, position, turbulence, pitch-to-diameter ratios, and Reynold's number. Q. Iqbal and S. Khushnood identified and quantified different damping mechanisms. They emphasised the thermal characteristics of damping mechanisms exposed to single-phase-based cross-flow in the shell and tube-type heat exchangers and developed a safer design based on experimental and empirical relations [14]. In the present study, tube internal velocity has been varied with varying shell-side velocity to analyze the vibration response of tube in the third row. Both drag and lift direction amplitudes were analyzed. This is the first experiment of its kind that offers insight into the vibration behavior of glass tubes with varying internal tube flow velocity in the shell and tube heat exchanger.

EXPERIMENTAL SETUP

A shell and tube-based real heat exchanger was developed using glass (borosilicate). It was coupled with a low-velocity closed-loop water test rig as shown in Fig. 1. A 200 gallons water storage tank was connected such that it acted as a buffer for both the continual loops i.e. outer shell side and tube side flows. A 7HP pump was mounted to achieve a range of flow velocities from 0.5 ms^{-1} to 2 ms^{-1} on the shell side and a 3HP pump was incorporated to produce a flow velocity range of 0.212 to 0.371 ms^{-1} on the tube side. The bypass valves were installed to regulate the water flow rate and velocity at both inlets. The Doppler flowmeter was mounted at the intake pipe just before the tube bundle to measure the flow velocity. The reduced velocity range was from 1.0225 ms^{-1} to 4.0901 ms^{-1} and Reynold's number ranged from 44500 to 66000. Unlike the usual practice of placing honeycomb flow straighteners on the shell side inlet to maintain a uniform flow; no flow straighteners were used in this experimentation. The vibrational response of the monitored tube could be a little different when there is a uniform flow in the tubes but the leading flow regime was somewhat similar. In this case, turbulence is because of the range of the reduced velocity. Table 1 shows the design parameters of the heat exchanger and the tube bundle that are utilized in this study. Figure 1 shows the experimental setup used

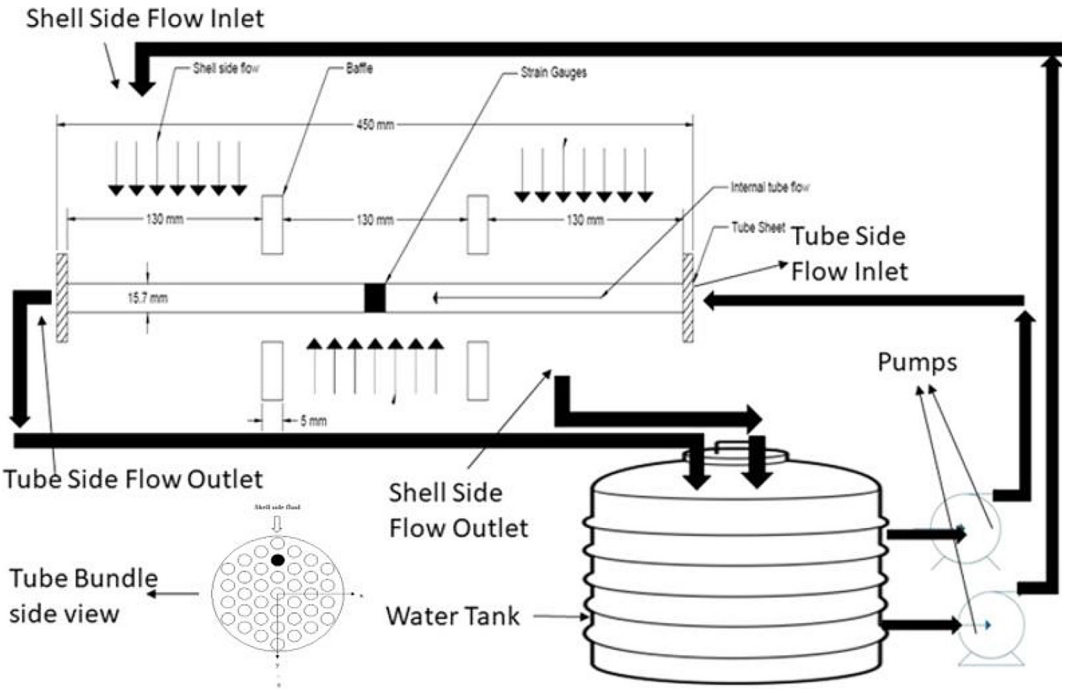

Figure 1. Heat exchanger setup layout

in this research. Figure 2b shows the tube bundle cross-section. The instrumented/monitored tube in the bundle is indicated with a black circle. The strain gauges were mounted on the instrumented/monitored tube by using a full Wheatstone bridge construction principle, with one gauge parallel to the direction of the flow and the other one perpendicular to it as depicted in Figure 2a.

The strain gauges were installed on the monitored tube using wired connections to capture the tube's vibrational response in stream-wise direction (lift) as well as in transverse flow direction (drag). The examined tube was positioned in the tube bundle's third row as shown in Figure 2b. One end of the tubes had a baffle and the other end had a tube sheet. Therefore, the tubes have a fixed damped boundary.

Figure 3 presents monitored tube's schematic diagram. The strain gauges were installed on the tube using the full Wheatstone bridge construction principle and attached to wireless sensing SG-Link at the node; made by MicroStrain Corporation, USA. The strain gauge measured the tube strain and transformed it into displacement. These displacements were presented in the form of a signal i.e. displacement as a function of time. Wireless sensors were embedded in the system to fetch data from the test rig. The wireless sensors give more accurate results with less distortion and noise as compared to the wired sensor. The entire data acquisition system is presented in Figure 4.

Table 1. Specifications of tube bundle heat exchanger

Shell and tube material	Glass
No. of tubes	37
Tube arrangement (Parallel and triangular)	(60°)
Mass of the tube	98 g±0.1g
Outer & Inner diameter of the tube	15.7 mm & 11.7 mm
No. of baffles	2
Baffle holes clearance	0.5 mm
Shell and baffle clearance	5 mm
The tube side fluid & its temperature	Water/22°C
The shell side fluid & its temperature	Water/22°C
No. of spans	3 (Unequal spans)
Length of monitored span	204 mm
Strain gauge's location	Mid-span
Tubular pitch	22.7 mm
Pitch to dia. Ratio	1.44
Elastic Modulus (glass tube)	60 GPa
Tube material density (glass)	2500 kg/m^3

As shown in Figure 4 the SG-Link wireless sensor was linked to the WSDA wireless base station. The PC was directly linked to the base station using Node Commander software. This software generates the real-time graph of the output signal. The data were collected at the rate of 736 samples per second. SIGVIEW was utilized for data mining and interpretation. Signals from the sensor using SIGVIEW software RMS amplitude were calculated at three different points, and then the average value was considered for lift as well as drag. The resultant RMS amplitude was calculated from both lift and drag values by Eqs. 5 and 6.

$$Amplitude\ RMS = Amplitude\ Peak/\sqrt{2} \quad (5)$$

$$R = \sqrt{(Lift\ RMS)^2 - (Drag\ RMS)^2} \quad (6)$$

RESULTS AND DISCUSSION

Vibrational response

The amplitude of tube bundle vibration is a primary concern to address in the cross-flow arrangement [6]. In this study, the vibrational tendencies of the monitored tube are observed during two distinct flow conditions. For the first condition, the velocity of the variable flow inside the tube ranged from 0.212 m/s to 0.371 m/s and in the second condition, there was no flow. The magnitude of shell side velocity in both cases was between 0.5 m/s and 2 m/s. The response of the monitored tube for both conditions is shown in Figure 5.

As shown in Figure 5 the tube's response for both stream-wise and transverse directions varies significantly; as the shell side velocity increases under different flow conditions. The RMS amplitude (measured as a percentage of the tube's outer diameter) in the transverse direction was relatively higher than that in the streamwise direction. The RMS amplitude increased considerably with the rise in shell side velocity at 2 m/s. There was no substantial increase in RMS amplitude up to 1 m/s. The rising RMS amplitude pattern is almost linear.

Figure 6 shows the vibrational response of the tube when the shell side flow velocity varies

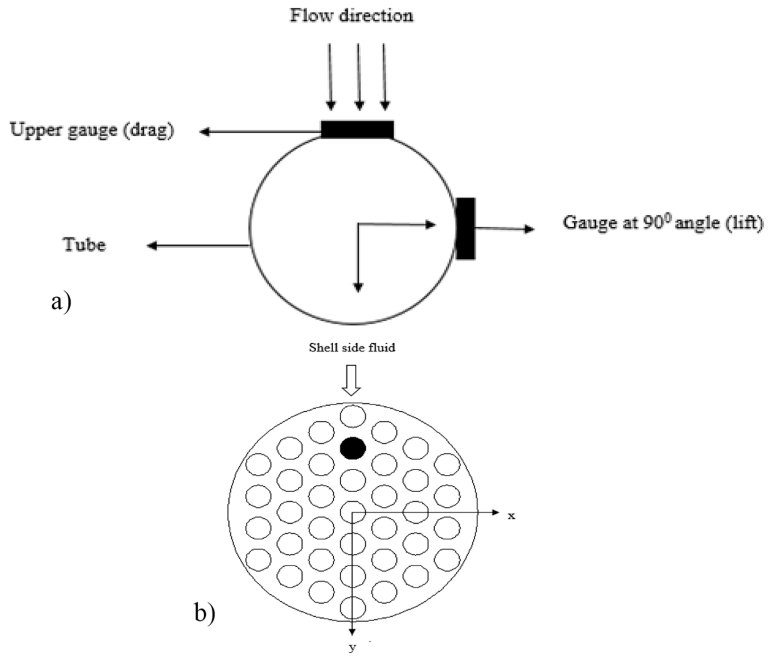

Figure 2. (a) Monitored tube showing the location of strain gauges w.r.t the direction of flow (b) tube bundle cross-sectional view (black circle shows the monitored tube)

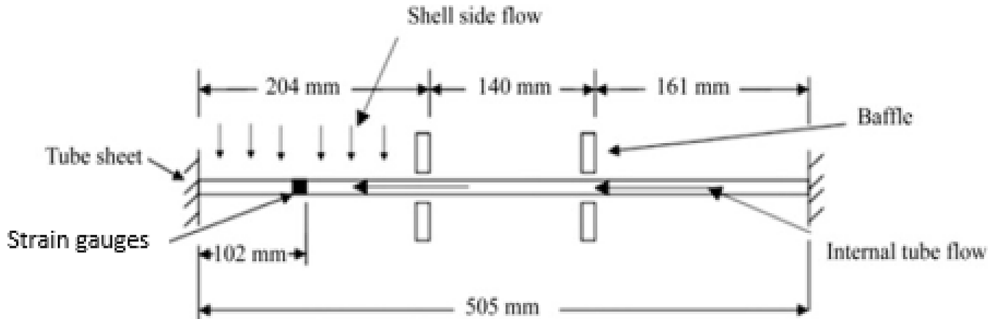

Figure 3. Test tube diagram showing the direction of the tube and the position of the strain gauges

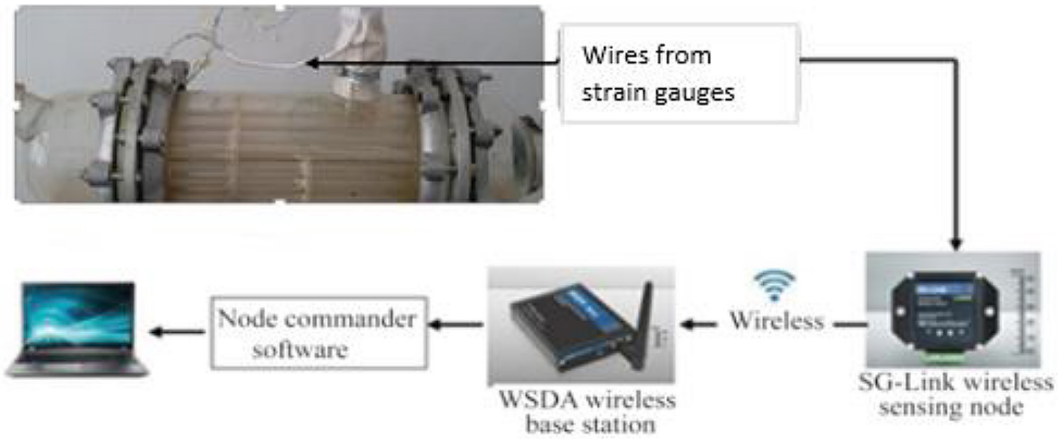

Figure 4. Data acquisition loop

from 0.5 m/s to 2 m/s while the tube side velocity is in the range from 0.212 m/s to 0.371 m/s. As the shell side velocity rises, the RMS amplitude increases. It has been observed that the amplitude of transverse vibrations is higher than in the stream-wise direction. The response of the monitored tube is quite identical and minimal in both directions i.e. stream-wise and the transverse

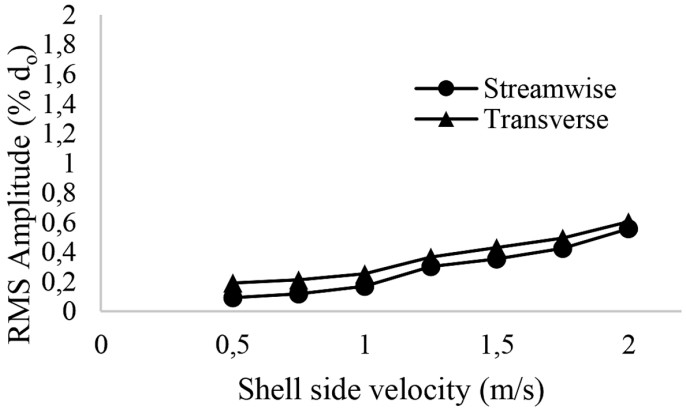

Figure 5. Monitored tube vibration response without side tube flow

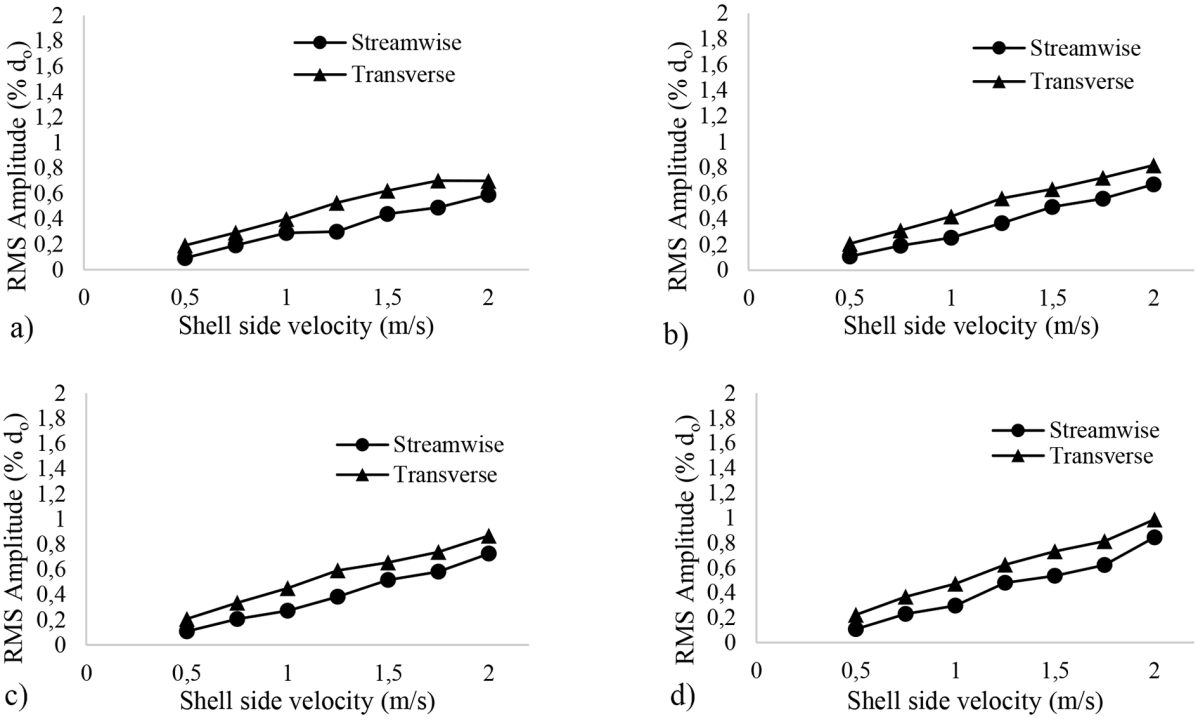

Figure 6. Monitored tube vibration response with a tube flow velocity of (a) 0.212 m/s (b) 0.265 m/s (c) 0.318 m/s (d) 0.371 m/s

when there is no internal flow but when there is an internal flow, the tube oscillates at relatively higher amplitudes. The reason is that the flow through the inner tube raises its mass during oscillations, thus generating an increased vibrational amplitude upon excitation from the shell-side fluid flow [15]. The increasing trend is quite linear for the free stream velocity range of 0.5 m/s to 2 m/s. It has been observed that the RMS amplitude escalates in both transverse and stream-wise directions when the tube side velocity increases. It is obvious from the experimental results that the addition of mass to the vibrating tube body enhances overall tube vibrations for the specifications considered in this study.

The vibrational response against different velocities of both the shell side and the tube side is presented in Figure 7. The vibrational response gets around four times higher when the shell side velocity goes up from 0.5 m/s to 2 m/s against the tube side velocity of 0.212 m/s and the response gets even higher (around five times) against the tube side velocity of 0.371 m/s. As the internal tube flow increases the amplitude also increases because of the mass addition. This additional mass effect the vibrational response of the tube. It is quite significant at the maximum tube and maximum shell side velocity as the amplitude is slightly higher than the usual trend at that particular point in the graph.

In Figure 8 the vibrational response against different tube flow velocities is plotted and a comparison is made with the findings of Khushnood. S. and Nizam, L.A. [16]. This comparison depicts that as the velocity of the tube side increases, the vibrational amplitude also increases. Khushnood. S. and Nizam. L.A. experimentation had a constant tube side velocity of 0.1 m/s whereas the current study incorporates a variable velocity (0.212–0.371 m/s).

Damping

A mechanism devised for energy dissipation from a vibrating body is called damping. The system's damping strongly influences the amplitude of the vibration. The amplitude of vibration decreases because of energy extraction. Mostly the heat exchangers possess quite a small damping magnitude [8]. The vibration frequency rises significantly in FIV which means that a lot of energy is added to vibrating tubes that can't be dissipated by the small damping. In this study, the damping ratio is projected using the bode plot as was done by S. Khushnood [17]. The logarithmic decrement was found using the mathematical relations presented in the form of Eqs. 7 and 8.

$$\zeta = {f_2 - f_1}/{2f_n} \tag{7}$$

$$\delta = {2\pi\zeta}/{\sqrt{1-\zeta^2}} \tag{8}$$

Where ζ represents damping ratio, δ depicts logarithmic decrement, and f_1, f_2 and f_n represents the frequencies mined using a bode plot. The logarithmic decrement determines how rapidly the amplitude of vibrating tubes will decay. The higher the damping ratio the faster the vibration amplitude decays [8].

Figure 9 shows the log decrement plot of the monitored tube in stream-wise and transverse directions for various tube flow velocities. Although a definite damping pattern is not observed against a rise in the free stream velocity. However, it seems to fluctuate around a uniform trend. The analysis reveals that the mean damping value becomes a bit higher as the tube flow velocity escalates. For instance, the mean value of logarithmic decrement is around 0.1 for no internal tube flow and around 0.15 for the maximum internal tube flow velocity of 0.371 m/s. The reason is an increase in the kinetic energy of the tube because of enhanced internal tube flow, which in turn produces more vibrations in the tube.

STABILITY ANALYSIS

A stability map for a single tube cylinder and a cylinder group (tube bundle) is one of the most important parameters for understanding instability. It is formulated in two non-dimensional parameters i.e. the mass damping parameter (MDP) and the reduced velocity as indicated in Eq. (9).

$$\frac{U_c}{f_n D} = K\left(\frac{m\delta}{\rho D^2}\right)^b \tag{9}$$

Roberts was the first investigator to examine the elastic instability of cross-flow fluids and revealed that the tube displacement mechanisms can also be the reason for dynamic tube row instability. He carried out experiments on the cylinder rows of a wind tunnel and determined the values

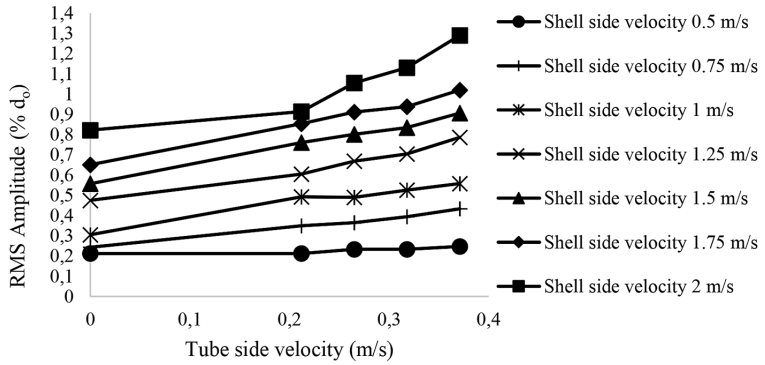

Figure 7. Vibrational response of the monitored tube (shell side amplitude)

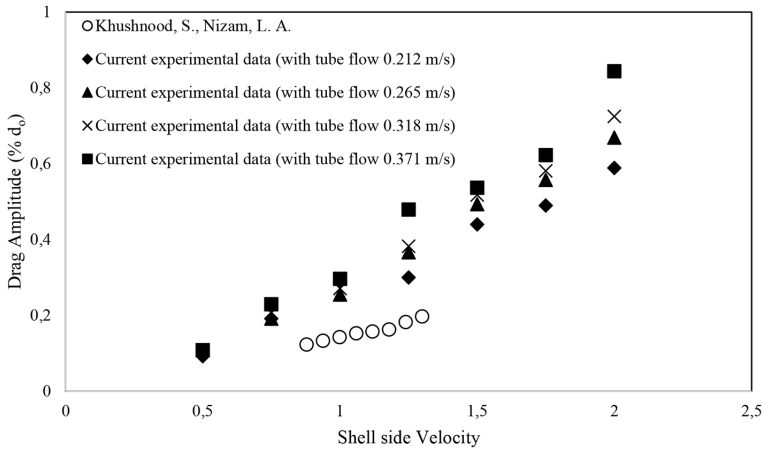

Figure 8. Comparison of vibration amplitude experimental results with Khushnood. S., Nizam, L.A.

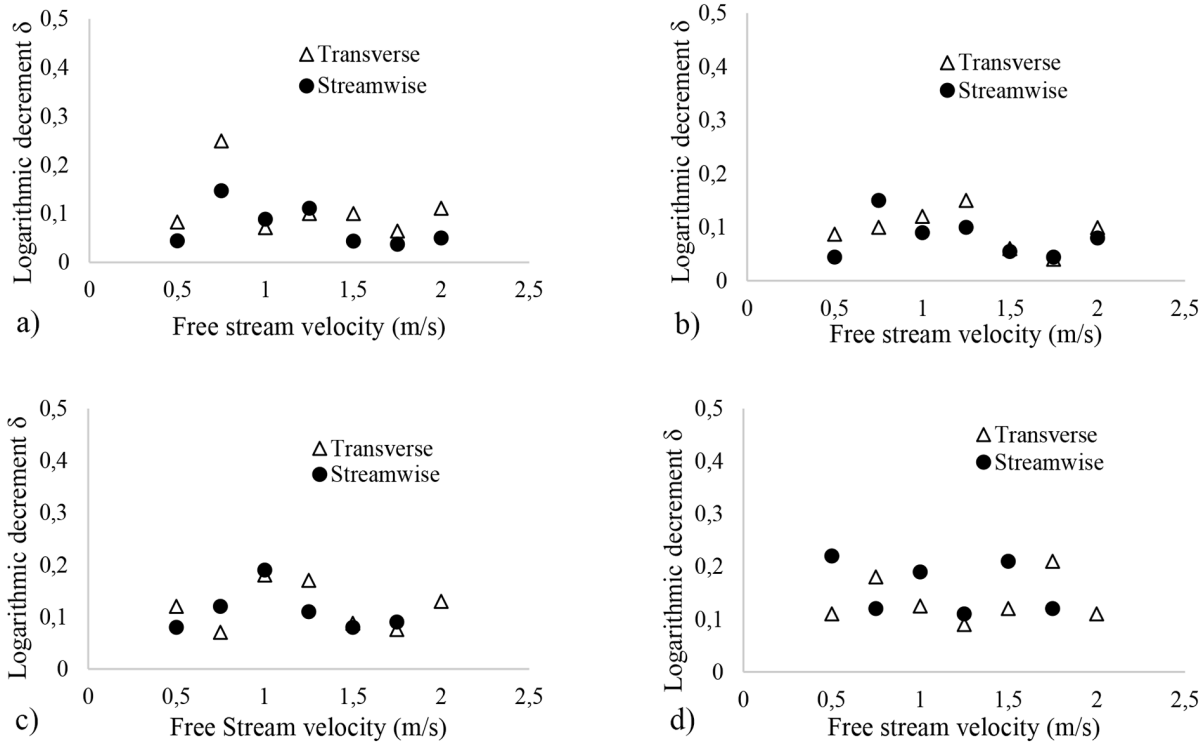

Figure 9. Logarithmic decrement (a) without tube side velocity (b) with tube side velocity 0.212 m/s (c) with tube side velocity 0.265 m/s (d) with tube side velocity 0.371 m/s

of K = 9.8 and b = 0.5. Connors also studied elastic fluid instability inside the tube bundle of heat exchangers and found the K (Connor's Constant) value to be 9.9 which is quite close to the Roberts result. The researchers studied fluid elastic instability in depth using different geometric parameters to develop improved guidelines for safer tube bundle design to prevent heat exchanger failure.

Figure 10 presents a comparison of previously published experimental results of reduced velocity over a mass-damping parameter range of 0.05 to 1000. It includes the data acquired in different scenarios i.e. different configurations of the tube bundle in single-phase flow; heat exchanger tubes in open channel liquid flow, and the tube bundle in the wind tunnel. From the stability analysis for a tube flow velocity of 0.265 m/s, the data seems to be more scattered than other velocities and mostly lies above the theoretical boundaries. As the flow velocity is increased from 0 to 0.371 m/s, the data shows a clear shift towards the right side of the graph upon gradual velocity increments. The data moves from the theoretically stable boundary regions to an unstable region upon increasing the flow velocity. So, it is concluded that the flow rate is an important factor to be considered while

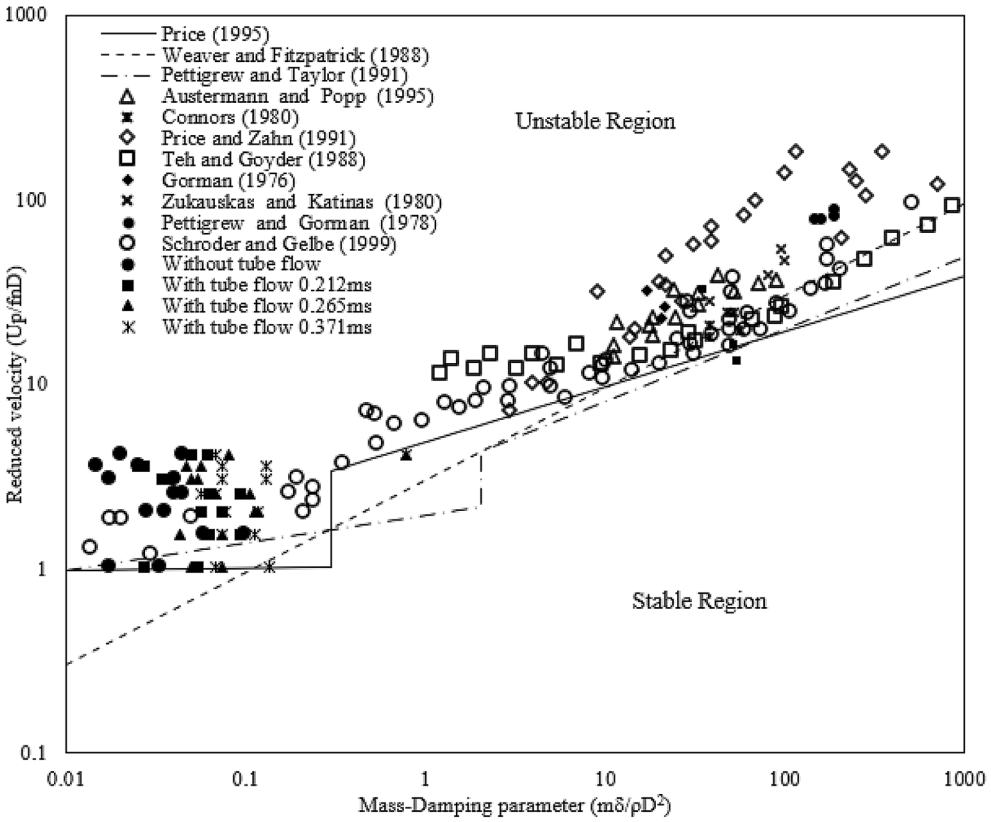

Figure 10. Stability maps for P/D ratio of 1.44

predicting the stability boundaries of the tube bundle and developing design guidelines.

CONCLUSIONS

The experimentation to investigate the influence of the internal tube flow velocity on the vibrational response of the monitored glass tube was carried out under different shell side velocities. The subsequent conclusions can be drawn after analyzing the results of this study. With an increase in the flow velocity of the shell side fluid, the vibration amplitudes of the tube increase gradually but remain below 1.5% of the tube's outer diameter. This stipulates that the principal excitation source in the tubes is turbulence buffeting.

With a rise in the tube side flow velocity, the tube's vibrational amplitudes start to increase gradually. The tube vibration amplitude for the highest shell side velocity is approximately 1.3% of the tube's outer diameter for the internal flow velocity of the overall tube. This is due to the increased vibrating mass of the tube as well as the internal flow fluctuations resulting in such vibrations. Logarithmic decrement (damping) analysis shows that the damping does not vary significantly instead it fluctuates around the consistent trend even for the higher internal tube and shell side velocities. It also indicates that the primary cause of excitation is turbulence buffeting. The data points tend to be present in the left portion of the stability map and particularly in the unstable region. The reason is that the theoretical models that were previously developed did not account for the internal tube flow velocity. So, there is a substantial deviation in the experimental outcomes as compared to the theoretical models. It leads us to a research gap that suggests making modifications in the current theoretical models to predict the realistic and more accurate stability behaviour of the tubes.

REFERENCES

1. Weaver D., Fitzpatrick J. A review of cross-flow induced vibrations in heat exchanger tube arrays†† The original version of this paper was prepared for presentation at the International Conference on Flow Induced Vibrations, Bowness-on-Windermere, 12–14 May 1987; proceedings published by BHRA The Fluid Engineering Centre, Cranfield, England (ed. R. King). Journal of Fluids and Structures. 1988; 2(1): 73–93.

2. Price S. A review of theoretical models for fluidelastic instability of cylinder arrays in crossflow. Journal of Fluids and Structures. 1995; 9(5): 463–518.
3. Chen S. Guidelines for the instability flow velocity of tube arrays in crossflow. Journal of Sound and Vibration. 1984; 93(3): 439–455.
4. Roberts B.W. Low frequency, aerolastic vibrations in a cascade of circular cylinders: Institution of Mechanical Engineers; 1966.
5. Lin T.K., Yu M.H. An experimental study on the cross-flow vibration of a flexible cylinder in cylinder arrays. Experimental thermal and fluid science. 2005; 29(4): 523–536.
6. Connors H. Fluidelastic vibration of heat exchanger tube arrays. Journal of Mechanical Design. 1978; 100(2): 347–353.
7. Blevins R. Fluid damping and the whirling instability of tube arrays. Flow-Induced Vibrations. 1979: 35–9.
8. Blevins R.D. Flow-induced vibration. New York, Van Nostrand Reinhold Co, 1977; 377.
9. De Paula A., Endres L., Möller S. Bistable features of the turbulent flow in tube banks of triangular arrangement. Nuclear Engineering and Design. 2012; 249: 379–387.
10. Usman M., Khushnood S., Nizam L.A., Tanveer W., Shafi A., Ayub M., et al. Investigation of the Effects of the Incident Flow Angle on Vibration Behavior in Heat Exchanger Tube Bundle. Advances in Science and Technology Research Journal. 2019; 13(2).
11. Ali N., Khushnood S., Nizam L.A., Bashir S., Hafeez A. Experimental investigation of the internal tube flow effect on the vibration response of tubes in a shell and tube heat exchanger. Transactions of the Canadian Society for Mechanical Engineering. 2020; 45(2): 211–220.
12. Grotz B., Arnold F. Flow-induced vibrations in heat exchangers: Stanford University, Department of Mechanical Engineering; 1956.
13. Lienhard J.H. Synopsis of lift, drag, and vortex frequency data for rigid circular cylinders: Technical Extension Service, Washington State University; 1966.
14. Iqbal Q., Khushnood S. Techniques for thermal damping in tube bundles. Mehran University Research Journal of Engineering & Technology. 2009; 29(4): 635–646.
15. Weaver D., Yeung H. The effect of tube mass on the flow induced response of various tube arrays in water. Journal of Sound and Vibration. 1984; 93(3): 409–425.
16. Khushnood S., Nizam L.A. Experimental study on cross-flow induced vibrations in heat exchanger tube bundle. China Ocean Engineering. 2017; 31(1): 91–97.
17. Khushnood S. TH-SOF-0475-Vibration analysis of a multi-span tube in a bundle: Nust. College of Electrical & Mechanical Engineering; 2005.